

WINTHROP UNIVERSITY  
SUMMER UNDERGRADUATE RESEARCH EXPERIENCE (SURE)  
2013 ABSTRACT BOOK



WINTHROP  
UNIVERSITY



## Table of Contents

<b>Student</b>	<b>Faculty Mentor</b>	<b>Page</b>
Adaeze Aninweze	Birgbauer, Biology	4
Kenisha Barber	Harris, Chemistry	5
Lucas Boncorddo	Grossoehme, Biochemistry	6
Kendra Bufkin	Sumter, Biochemistry	7
David Burlinson	Grossoehme, Biochemistry / Doman, Computer Science	8
Keisha Carden	Lammi / Hanna, Chemistry	9
Spenser Cote	Werts, Geology	10
Lissa DiSparano	Hartel, Chemistry	11
Tyra Douglas	Harris, Chemistry	12
Esseabasi Etim	Lammi, Chemistry	13
Hannah Hadaway	Evans-Anderson, Biology	14
Katja Hall	Calloway, Chemistry	15
Stephanie Henry	Grattan, Chemistry	16
Hua-Wu Huang	Sumter, Biochemistry	17
Matthew Ingersoll	Grossoehme, Biochemistry	18
Grace Jones	Glasscock, Biology	19
Taisha Jones	Gelabert, Chemistry	20
Kristen McLaurin	Lammi, Chemistry	21
Jesse Mclaughlin and Ashley Williams	Grossoehme, Biochemistry	22
Briana Milks	Hurlbert, Biochemistry	23
Louise Mount	Grattan, Chemistry	24
Jamie Murakami	Hanna, Chemistry	25
Briana Murray	Hurlbert, Biochemistry	26
Denise Peppers	Grossoehme, Biochemistry	27
Emili Price	Rusinko, Mathematics	28
Alec Reed	Hurlbert, Biochemistry	29
Derion Reid	Sumter, Biochemistry	30
Mariam Salib	Hurlbert, Biochemistry	31
Hannah Swan	Rusinko, Mathematics	32
Velma Tahsoh	Calloway, Chemistry	33
James Vinton	Birgbauer, Biology	34
Justin Waller	Harris, Chemistry	35
Sarah Wicks	Hanna, Chemistry	

## ACKNOWLEDGEMENTS

*The undergraduate abstract authors were supervised by a vibrant group of faculty in the Biology, Chemistry, and Mathematics Departments. On behalf of the students, faculty, and department administrators, we express our gratitude for the support from the agencies and organizations listed below. The hands-on teaching experiences that faculty provide for these outstanding Winthrop students are only possible through their support.*



American Chemical Society



National Science Foundation  
WHERE DISCOVERIES BEGIN



Carolinas HealthCare System

*Uncompromising Excellence. Commitment to Care.*



WINTHROP  
UNIVERSITY



## **Ibuprofen Induces Growth Cone Collapse in Embryonic Retinal Axons**

**Adaeze Aninweze (2016)**

**Mentor: Dr. Eric Birgbauer**

Damage to the CNS and the spinal cord is irreversible. There is minimal nerve regeneration at the site of the injury, but it is not enough to reverse the injury. Fu et al (2007) found that ibuprofen promoted axon regeneration via RhoA inhibition in dorsal root ganglion cells of mice. RhoA prevents nerve regeneration, but ibuprofen was found to inhibit RhoA allowing the nerves to regenerate. Similarly, RhoA is found in the embryonic retinal axons of chicken embryo. In the retinal axons of chicken embryo, LPA causes growth cone collapse through the RhoA pathway. If ibuprofen promoted axonal regeneration through RhoA inhibition, growth cone collapse in retinal axons of chicken embryo by LPA should be hindered by ibuprofen preventing growth cone collapse. The ibuprofen treatments used by Fu et al were used to treat the retinal axons of the chicken embryo. Two concentrations of ibuprofen, 500 $\mu$ M and 50 $\mu$ M, and 100nM LPA were used to treat the retinal axons. Time-lapse microscopy was used to record live events as the retinal axons were treated with treatments of ibuprofen and LPA. After LPA treatment, retinal axons pretreated with 50 $\mu$ M Ibuprofen saw 71.4% growth cone collapse and 88.9% growth cone collapse when pretreated the 500 $\mu$ M Ibuprofen. Thus, ibuprofen did not prevent growth cone collapse after LPA treatment. Furthermore, treatment with 500 $\mu$ M concentration of ibuprofen caused growth cone collapse on its own. These findings were opposite to Fu et al findings that ibuprofen promoted axon regeneration.

*Support was received from Winthrop University and from a National Institute Health Grant from the National Center for Research Resources for the support of the program entitled "South Carolina IDeA Networks of biomedical Excellence" (SC-INBRE).*



## Photooxidation of Water Using $\text{WO}_3/\text{RuO}_2$ Thin Films

**Kenisha Barber**

**Mentor: Dr. Clifton Harris**

$\text{WO}_3$  is a semiconductor suitable for water oxidation due to its valence band potential being more negative than the oxidation potential of water. Since it is also a visible light absorber, sunlight can be used as the driving force. The objective of this research was to create a  $\text{WO}_3/\text{RuO}_2$  thin film system that can use solar energy to oxidize water.  $\text{WO}_3$  nanoparticles were embedded into an  $\alpha$ -terpeneol based paste and applied to conductive glass substrates via a doctor blading technique. Ruthenium particles were synthesized using reverse micelles of  $\text{RuCl}_3(\text{aq})$  and  $\text{NaBH}_4(\text{aq})$  in heptane. Surface charge is induced on Ru by functionalization of the particle surfaces with capping ligands, or by the generation of surface bound ions resulting from sufficiently acidic pH conditions of the confined aqueous media. These charged particles are electrodeposited onto the  $\text{WO}_3$ -coated substrate and annealed in air to obtain the oxide, as illustrated in figure 1. This photooxidation catalyst will be paired with a photoreduction catalyst to theoretically yield a self-sustained water-splitting device.

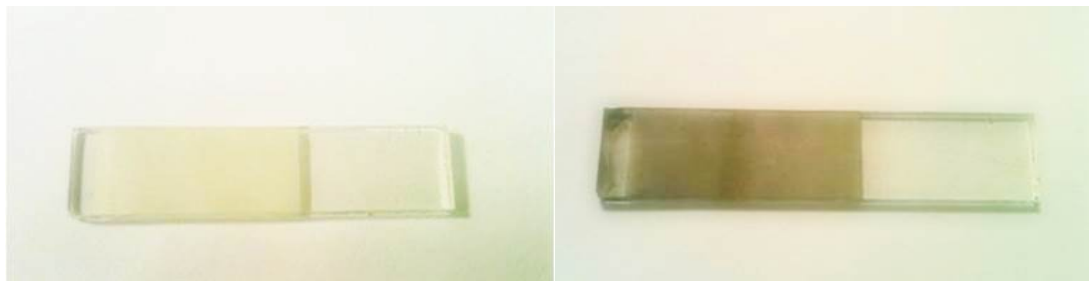


Figure 1. UV-Vis Absorbance Spectra of Gold NS (left) and NR (right) with various ratios of precursor to capping agent.

*This research was supported by the Winthrop University Research Council SC13010.*



## Preparation for *Ciona intestinalis* FoxO Chromatin Immunoprecipitation Assay

**Lucas Boncorddo (2015)**

**Mentor: Dr. Nicholas Grosseohme and  
Dr. Heather Evans-Anderson**

Recent research has identified *Ciona intestinalis* as a model organism for heart regeneration. FoxO is an important protein in the life cycle of *Ciona intestinalis*. Human FoxO1 and *Ciona intestinalis* FoxO1 share an area of high similarity in amino acid residues. This area corresponded to the Forkhead DNA binding region of FoxO1. Previous in vitro experiments in our lab have characterized the Protein-DNA interactions between FoxO and the known regulatory elements, insulin response element from humans and Daft-16 binding element from *Drosophila melanogaster*. However, these DNA sequences are not found in the *Ciona* genome. Therefore, we sought to identify the sequences of DNA that FoxO binds to in vivo and express FoxO endogenously. To do this we utilized the Chromatin Immuno-Precipitation Assay (ChIP Assay) to identify the sequences of the *Ciona intestinalis* genome that FoxO binds to. For the ChIP assay, we opted to make use of the readily available antibody that recognizes hexahistidine tagged proteins. While *Ciona intestinalis* naturally expresses FoxO, it is not hexahistidine tagged. Using standard cloning techniques, a hexahistidine tagged FoxO DBD was inserted into a pCes, *Ciona* expression system, expression plasmid developed by colleges at Stanford. Once confirmed by sequencing, the expression plasmids were then electroporated into *Ciona* *intestinalis* embryos. Once FoxO is successfully expressed by *Ciona* *intestinalis* a ChIP Assay will be performed.

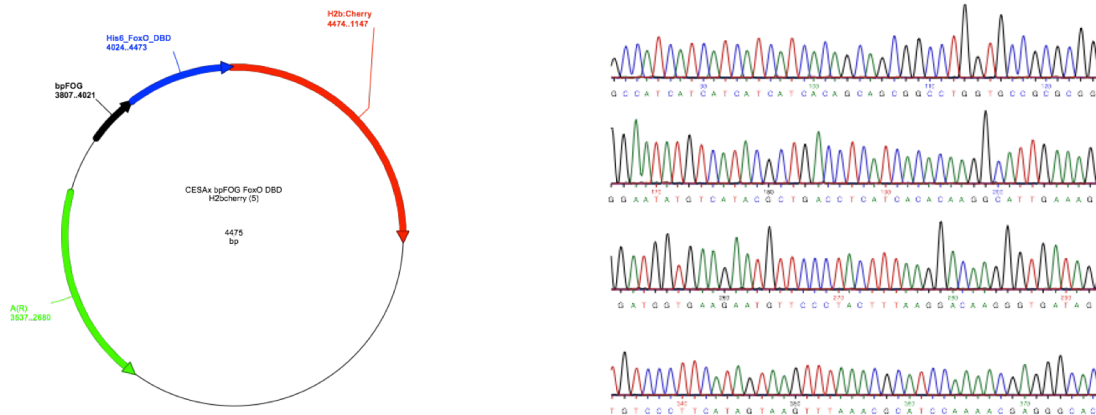


**Figure 1: pCES:foxO\_DBD vector design and electropherogram confirming the sequence integrity of the *foxO* gene insert between the native FOG promoter and the H2b.Cherry reporter gene.**

*Support for this research was provided by INBRE-III, NIH grant (1R15HL104857-01), HEA) Winthrop University Department of Biology, and the Winthrop University Department of Chemistry, Physics and Geology.*

## Replacement of a Conserved Arginine at Position 25 in High Mobility Group A1 Proteins Affects DNA Binding Affinity

Kendra Bufkin (2015)

Mentor: Dr. Takita F. Sumter

The chromatin binding proteins, High Mobility Group A1a and A1b (HMGA1a/b) possess a characteristic Arginine-Glycine-Arginine (RGR), that selectively binds AT-rich DNA to initiate neoplastic transformation. These proteins are master regulators of cancer initiation and are subject to covalent modifications that may serve as prognostic markers for cancer. Because of their DNA binding ability, HMGA1 proteins can regulate gene expression of other cancer-causing genes; likely providing new targets for cancer treatments. In cancer, arginine within the characteristic sequences of HMGA1's AT-rich DNA binding domains has been chemically modified to bear one or two methyl groups at the center of each DNA binding domain. This modification likely changes the protein's structure and modulates DNA binding. We are evaluating the DNA binding of an HMGA1 variant whereby an Alanine (A) is substituted for R (R25A) in order to determine if the absence of Arg impacts DNA binding of HMGA1. We hypothesize that the Arginine 25 residue within the first AT-hook of HMGA1 is important to the interaction between HMGA1 and AT rich DNA sequence. Our preliminary fluorescence data confirms previous studies in which DNA binding is compromised upon substitution of R25. Furthermore, these findings are consistent with recent crystallography data demonstrating the potential impact of arginine methylation on DNA binding. Better understanding the role of chemical modifications of HMGA1 will be critical to improvements in cancer-targeted therapies.

Table 1. Calculated Dissociation Constants

	DNA alone	HMGA	R25A HMGA
Maximal Binding ( $B_{max}$ )	3335	2622	2454
DNA Dissociation Constant ( $K_d$ , $\mu M$ )	0.4098	0.2365	0.2599
Percent change of $K_d$		42.2%	36%

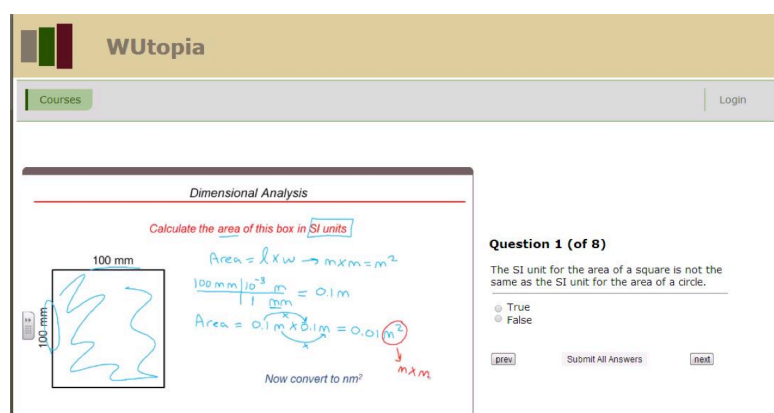
*This work was supported by grants from the NCI (1R15CA137520-01 and NIGMS(8 P20 GM103499) of the National Institutes for Health, the National Science Foundation (MCB0542242) with student support from the Winthrop McNair Scholars program.*

## Coordinating technologies in online and hybrid courses to stimulate engagement and retention

David Burlinson (2014)

Mentor: Dr. Nicholas Grosseohme and  
Dr. Marguerite Doman

Development of electronic educational technologies for online instruction has become a major goal of many universities. These materials include question/answers (data), lecture (video), problems (textual input), and others. The instructional delivery of an online course can overlap many of these artifact types. These artifacts, designed to heighten student involvement, can clutter the screen adding distraction. There is a challenge in concurrently presenting similar concepts of different artifacts in a meaningful way. The temporal constraint of stored or streamed video is managed differently than the retrieval of data for question/answer data type. To address this concern, we propose an ontological coordination of various and complementary course content artifacts in the online delivery. Using HTML5, AJAX, and Javascript, we linked a series of questions to timestamps in instructional videos on the website for a hybrid introductory Chemistry course at Winthrop University. As each video plays, the question pertaining to each segment of time and relevant topic is presented. To ascertain the effectiveness of such a dynamic presentation of course material, every page sends certain statistics and user data to a separate server for analysis, including but not limited to: whether students watch the entire video, the number of times students skip from question to question, and the amount of time spent on each question. We anticipate that not only the presence of the questions but specifically the coordination of the questions with the videos will provide an increase in engagement with and retention of the course material. As the successive semesters progress, we will refine the presentation of course material and the submission of relevant user data to effectively impact the tool for further enhancement of the chemistry course and eventual distribution for use in various other online/hybrid courses and information delivery systems.



The screenshot shows the WUtopia online learning platform interface. At the top, there is a header with the WUtopia logo and a 'Courses' menu. Below the header, there is a 'Dimensional Analysis' section with a problem: 'Calculate the area of this box in SI units'. The problem includes a diagram of a square with side lengths of 100 mm and 100 mm. Handwritten blue and red notes show the calculation:  $\text{Area} = l \times w \rightarrow m \times m = m^2$ ,  $100 \text{ mm} | 10^{-3} \frac{m}{\text{mm}} = 0.1 \text{ m}$ , and  $\text{Area} = 0.1 \text{ m} \times 0.1 \text{ m} = 0.01 \text{ m}^2$ . A note says 'Now convert to  $\text{nm}^2$ '. To the right of the problem, there is a 'Question 1 (of 8)' section with the text: 'The SI unit for the area of a square is not the same as the SI unit for the area of a circle.' Below this text are radio buttons for 'True' and 'False', and buttons for 'prev', 'Submit All Answers', and 'next'.

Figure 1: Screenshot of the WUtopia online learning platform as of August 26, 2013.

Support for this research was provided by Winthrop Research Council Grant (CE13006), Winthrop University Department of Computer Science and Quantitative Methods, and the Winthrop University Department of Chemistry, Physics and Geology.





## Mechanistic Insights into Small-Molecule Inhibitors of Amyloid- $\beta$ Aggregation

Keisha Carden (2014)

Mentors: Drs. Robin K. Lammi and James M. Hanna, Jr.

Amyloid- $\beta$  ( $A\beta$ ) is a peptide of 39-43 amino acids that self-associates into a diverse array of neurotoxic aggregates implicated in the memory loss and cognitive deterioration of Alzheimer's disease (AD). Inhibiting the aggregation process is therefore a primary research focus in the struggle toward AD prevention and treatment. Our group previously reported the synthesis and characterization of several small-molecule inhibitors (including 3,4-BPT, shown below), employing standard dye-binding assays to evaluate inhibitor efficacy. Chromophores such as Congo red (CR) and Thioflavin T (ThT) bind specifically to  $\beta$ -structured aggregates and thus permit indirect monitoring of  $A\beta$  aggregation, as unstructured monomers associate to form  $\beta$ -structured assemblies. We have now developed a dye-free, circular-dichroism (CD) based approach that facilitates investigations of inhibitors' modes of action through direct measurement of peptide structural transitions. Simultaneous CD and ThT measurements show nearly identical time courses for  $A\beta$  aggregation, including a single secondary structural transition from random coil to  $\beta$ -sheet that tracks closely with dye binding. While multiple Congo red and Thioflavin T assays confirm that 3,4-BPT significantly reduces the concentration of (dye-binding)  $A\beta$  aggregates present at equilibrium, CD results indicate that the peptide species present at equilibrium are  $\beta$ -structured. Preliminary transmission electron microscopy (TEM) measurements suggest that the equilibrium species formed in the presence of 3,4-BPT are structurally distinct from the fibril-like assemblies observed in control samples.

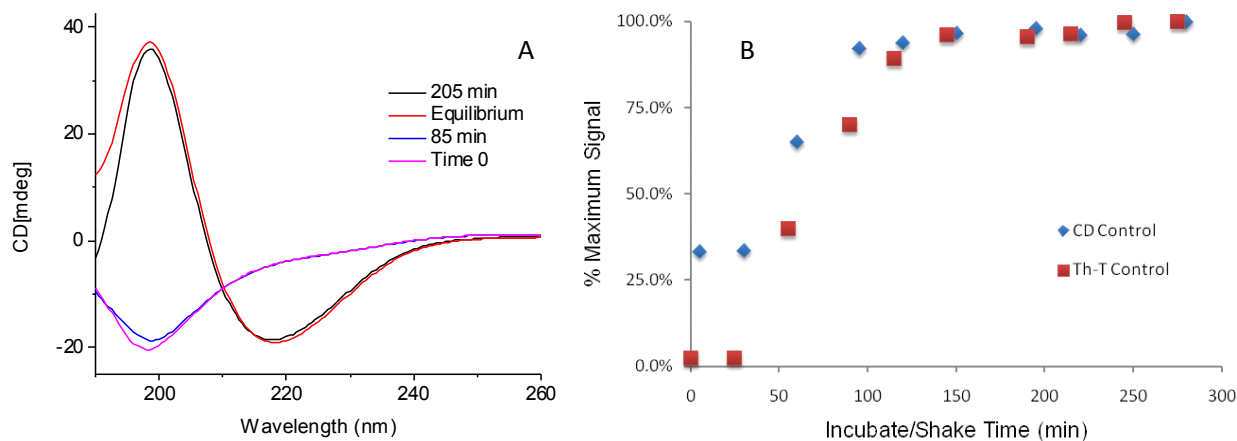


**Figure 1:** (A) Circular dichroism spectra of an  $A\beta$  sample depicting the development of  $\beta$ -sheet character (represented by minimum at 216 nm) over time. An isodichroic point near 210 nm confirms a single structural transition from random coil to  $\beta$ -sheet. (B)  $A\beta$  aggregation kinetics monitored by ThT dye-binding assay and CD secondary structural analysis. The two approaches yield very similar time courses.

*Support for this research was provided by the Winthrop University McNair Scholars Program and an NIH-INBRE grant from the National Center for Research Resources and the National Institute for General Medical Sciences.*

# Investigations of inorganic soil development in the peat of the Congaree Muck Swamp

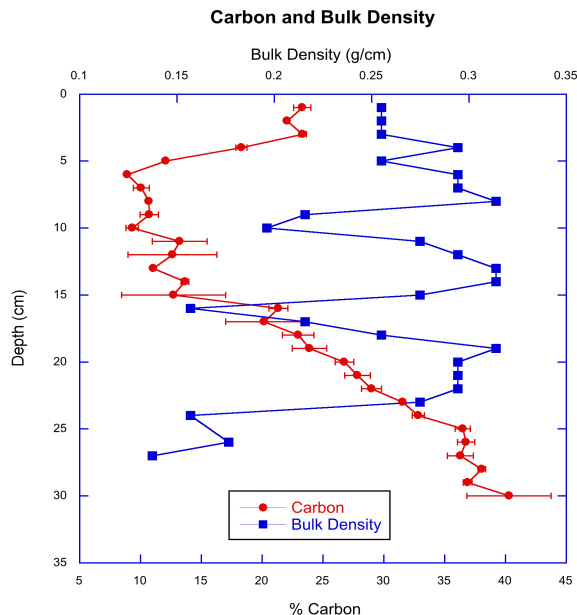
Spenser Cote (2013)

Mentor: Dr. Scott Werts

Congaree National Park, near Columbia, South Carolina, is a floodplain forest that contains the United States' largest contiguous track of old-growth bottomland forest as well as one of the highest natural canopies that remains on Earth. A portion of the park contains a groundwater fed muckswamp and is in the footprint of several ancient meanders of the Congaree River. Within one ancient meander lies an extensive peat deposit assembled over thousands of years from the formation of an oxbow lake. The aim of this study is to investigate the origin of an inorganic soil horizon forming near the surface of the peat at varying depths.

Initial exploration of the muckswamp area suggests that the inorganic layer is varying in

thickness throughout the swamp, becoming thicker in the center of the deposit. Because the layer is consistent through the area and lies a large distance from the river, we have been able to eliminate the possibility of flooding from the river and bioturbation as possible causes for the layer. Previous investigations into the stable isotopic signature of the carbon in the layer revealed consistent  $\delta^{13}\text{C}$  values throughout that layer (-28.0 to -28.5‰), suggesting that the cause is likely not high levels of decomposition within this layer.



due to the evapotranspiration processes of the vegetation. During the fall and winter, the water table rises again due to the plants going dormant and not drawing any water. As the water table rises, it likely dissolves some of the organic carbon in the upper layers of the soil. As the water table lowers again, the dissolved carbon is removed from the upper portions of the soil and transported out in the groundwater to nearby Cedar Creek. This research will aid in clarifying a major portion of the carbon cycle within this area and provide insight into the altered landscape seen in the muckswamp area.

*This project was supported by a grant from the Winthrop University Research Council and a grant from the Dalton Endowment.*



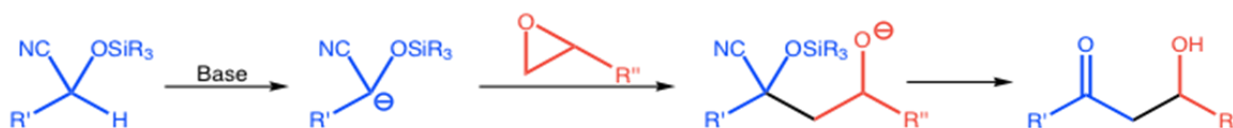
## The reaction of O-silylated cyanohydrin anions with epoxides as an alternative for the enantio- and diastereoselective preparation of aldols

Lissa DiSparano (2014)

Mentor: Dr. Aaron M. Hartel

The aldol addition is one of the most important carbon-carbon bond forming reactions in chemical synthesis. The traditional form of this reaction, between an aldehyde or ketone and a second enolized aldehyde or ketone, results in the formation of a  $\beta$ -hydroxycarbonyl (often referred to as an “aldol product”). The reaction can result in the formation of up to two new chiral centers, and the absolute and relative stereochemistry of the product can be challenging to control. Modern variations, especially those of Evans and related strategies, have allowed for significant enantio- and diastereoselectivity in the reaction. These methods, while extremely useful, have several drawbacks, including poor atom economy, use of expensive auxiliaries, and the additional synthetic steps required to introduce and remove these auxiliaries.

An alternative potential route for the enantio- and diastereoselective preparation of aldol products is the reaction of O-silylated cyanohydrins anions with epoxides. This method would take advantage of the wealth of excellent asymmetric epoxidation procedures available, providing an efficient method for the stereoselective formation of aldols.



A series of O-silylated cyanohydrins were prepared using established chemistry. These substrates were treated with LiHMDS to form the O-silylated cyanohydrin anions, which were subsequently alkylated with 1,2-epoxybutane. The newly formed adducts were then desilylated in order to expel cyanide and form the desired aldol product. Yields up to 84% for the two-step process (alkylation-desilylation) could be achieved. During the alkylating step, it was found that the amount of desired adduct formed was heavily dependent on the quenching technique employed. When small amounts of quenching agent (aqueous NH<sub>4</sub>Cl) were added to the reaction, the major product was a presumed cyclized imidate or lactone. The formation of this unwanted cyclized product could be minimized by slowly adding the reaction mass to a large excess of the quenching agent. Thus, a new method for the preparation of aldols has been discovered and will continue to be optimized and its scope investigated.

*Support was provided the Winthrop University Department of Chemistry, Physics, and Geology*



## Photocatalytic Reduction of Water Using CdSe/TiO<sub>2</sub>/Pt Thin Films

Tyra Douglas

Mentor: Dr. Clifton Harris

CdSe is a semiconductor suitable for the reduction of water due to the sufficiently negative potential of its conduction band relative to the reduction potential of water. The objective of this research was to create a CdSe/TiO<sub>2</sub>/Pt thin film for the catalytic conversion of solar light into H<sub>2</sub> (g). CdSe quantum dots were synthesized using reverse micelles as a stabilizing medium. The photo-reducing capability of CdSe was monitored using methyl viologen (MV<sup>2+</sup>) as a probe species. Later, the enhancement of this reduction was demonstrated by the coupling of CdSe with TiO<sub>2</sub>. To obtain CdSe/TiO<sub>2</sub>/Pt thin films, TiO<sub>2</sub> nanoparticles were platinized by a UV-treatment method, and these compound particles were then chemically linked to CdSe using a bifunctional linker molecule. This particulate agglomeration was then deposited onto fluorine-doped tin oxide (FTO) by electrophoretic deposition under high voltage (see figure 1). The evolution of H<sub>2</sub> following the irradiation of the catalyst film in aqueous has yet to be explored. If effective, the pairing of this photo-reduction catalyst with a photo-oxidation catalyst would theoretically yield a self-sustained water splitting device.

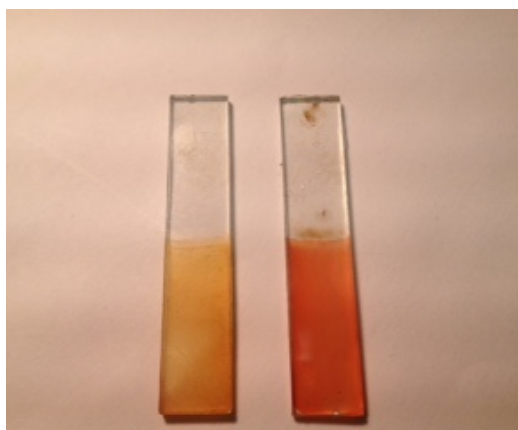


Figure 2. CdSe/TiO<sub>2</sub>/Pt thin film on FTO produced by electrophoretic deposition at 500V for 10 minutes. The differences in color are due to quantum size effects in CdSe.



## Improving Quantification of Amyloid- $\beta$ Oligomers: Automated Routines for Photobleaching Analysis

Esseabasi Etim (2015)

Mentor: Dr. Robin K. Lammi

Amyloid- $\beta$  ( $A\beta$ ) is a peptide of 39-43 amino acids that self-associates into neurotoxic assemblies linked to Alzheimer's disease. Recent studies show that the earliest oligomers, including dimers and trimers, may cause memory deficits. Our research harnesses the capability of single-molecule fluorescence spectroscopy to quantify these smallest oligomers, one at a time. For these studies, we employ  $A\beta$ 40 peptides with fluorescent (FAM) dyes attached to their N-termini and Lys-biotin groups attached to their C-termini. The biotin tags permit peptide assemblies to tether to functionalized cover slips; by exciting a single peptide species with laser light and observing the quantized photobleaching steps of its individual dyes, we are able to determine the number of associated peptides it contains. Until recently, much of this photobleaching analysis had been done by inspection – zooming in on fluorescence profiles and trying to determine how many intensity levels there were above background. We have now developed two additional tools to improve the efficiency and accuracy of this process. First, we have created an automated routine to generate photon-counting histograms (PCH) from fluorescence data. These plots depict the number of points observed with each particular number fluorescence counts, such that different intensity levels in the fluorescence profile should appear as distinct peaks in the PCH. Because these peaks often overlap, we have additionally developed a routine for automating the identification of photobleaching steps. This protocol is based on the idea that a discrete photobleaching step requires a significant decrease in fluorescence signal over a single time point, resulting in a large negative slope. By differentiating the acquired fluorescence intensity profiles and having the data-analysis software highlight points with the desired negative values, we can automate the location of likely photobleaching steps. We are currently in the process of evaluating these results for accuracy; upon validation, this routine will significantly speed up the process of quantifying oligomers, allowing for a much faster pace of research.

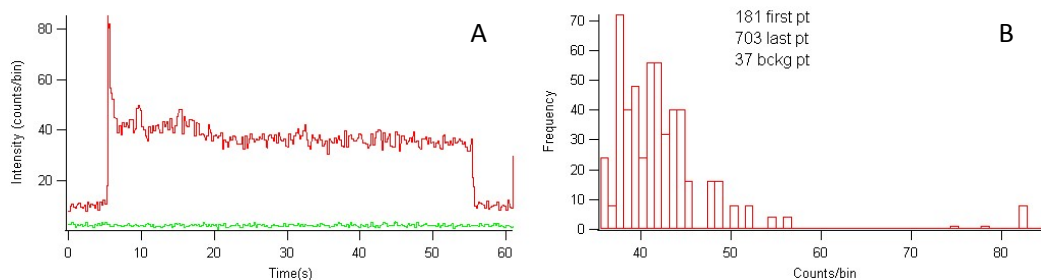


**Figure 1: (A) Fluorescence profile (in red) for an individual  $A\beta$  oligomer, after initial data processing. (B) Photon-counting histogram (PCH) generated from the profile in (A), showing two three intensity levels above background (as evidenced by two or three peaks centered above 40 counts).**

*Support for this research was provided by the NIH-INBRE grant from the National Center for Research Resources and the National Institute for General Medical Sciences.*

## **Validation of altered gene expression of FoxO1 and FoxO3 in endothelial cells**

**Hannah Hadaway**

**Mentor: Dr. Heather Evans-Anderson**

The goal of this project is to elucidate the role of the transcription factors FoxO1 and FoxO3 in the interaction between the endothelium and the myocardium during cardiovascular development. Previous work has shown the importance of FOXO1 in endothelial lineages during heart development (Sengupta, 2013). Specifically, loss of FoxO1 in endothelial cells leads to reduced proliferation in cardiac myocytes during heart development. The interactions between the endothelium and the myocardium during development are known to occur via cell-cell interactions as well as via diffusible cell signaling factors; however, the mechanism regulating cardiac myocyte proliferation is unknown. In order to replicate the *in vivo* phenotype, we used RNA interference (RNAi) to silence FoxO1 and FoxO3 gene expression in cultured endothelial cells. Once transfection efficiencies using RNAi constructs were optimized, we used western blot analysis to validate altered gene expression. Our results show that FoxO1 protein production was significantly reduced in transfected cells. Future goals of this project include developing an *in vitro* co-culture model system of endothelial cells and cardiac myocytes to replicate cell signaling during development. We will co-culture RNAi-treated endothelial cells with cardiac myocytes in order to determine differences in cell proliferation and apoptosis. The development of a co-culture model system for endothelial cells and cardiac myocytes will aid in the identification of the specific cell signaling factors involved in endothelial-myocyte interactions, which will provide valuable information that will have a greater impact on further research projects.

*The project described was supported by NIH Grant Number P20 RR-16461 from the National Center for Research Resources for support of the program entitled "South Carolina IDeA Networks of Biomedical Research Excellence" (SC-INBRE) and NIH Grant Number 1R15HL104587-01 from the National Heart, Lung, and Blood Institute.*



## Instrumental Developments for Chromium Emission with a Tungsten Coil Atomizer

Katja Hall (2016)

Mentor: Dr. Clifton Calloway

Tungsten coil atomic emission spectrophotometry (WCAES) is a dependable way to visualize chromium emission. The WCAES spectrophotometer is smaller than commercial inductively coupled plasma optical emission spectrophotometers (ICP-OES), using a commercially available tungsten bulb as the emission source and Ocean Optics CCD spectrophotometer to detect emission signals. The WCAES requires less power, no water-cooling and much less argon gas than commercial ICP-OES.

However, Calloway et al.'s device displays a significant level of background emission from the coil, limiting the dynamic range of chromium concentration detection. By adding an iris to the optical system, just before the entrance slit to the spectrophotometer, and modifying standard procedures for WCAES analysis, we expect the level of background emission on spectra to be reduced, improving detection limits and linear dynamic range. Optimum position will be determined by calculating and tracking the changes in the signal-to-noise ratios of each spectra as well as performing a calibration curve for the system once all changes have been made and the position of the iris optimized.

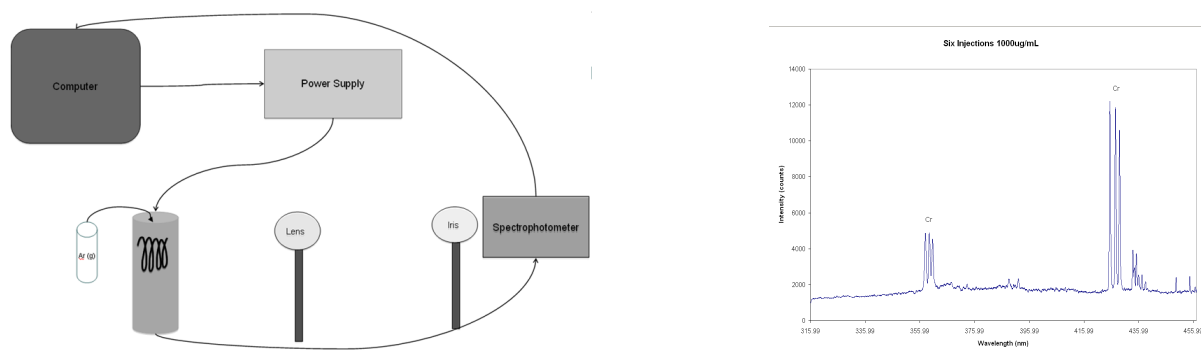


**Figure 1: Tungsten Coil Atomic Emission Spectrophotometer.** A pinhole iris added to reduce background emission from the coil for the determination of chromium concentration.

*Support for this research was provided by the Winthrop University NIH-EagleSTEM program and the Winthrop University Department of Chemistry, Physics and Geology.*



## **Design and Synthesis of Zone 4 Modified Sphingosine Kinase Inhibitors**

**Stephanie Henry**

**Mentor: Dr. Christian Grattan**

Sphingosine Kinase 1 (SK1) is an enzyme overexpressed in cancerous cells which regulates tumor growth; in healthy cells it controls proliferation and cell growth. SK1 is responsible for catalyzing the phosphorylation of sphingosine, which creates sphingosine-1-phosphate (S1P). S1P is a bioactive lipid that regulates proliferation, survival, and motility. The concentration of S1P and ceramide together regulate whether a cell can proliferate or be apoptotic. The enzymes in this pathway give to us pathways in which we may have new anticancer drugs. So far there have been several drugs that have inhibited SK1; however, they were nonselective and also inhibited other kinases that are important in other biochemical processes. A few inhibitors have been identified that are selective and inhibit cancer cell proliferation and stimulate apoptosis, which reduces the levels of S1P. The main goal of this project is to design, synthesize, and characterize pure, potent and selective derivatives of the SK1 template inhibitor that may be orally bioavailable. Specifically, I have successfully synthesized three pure compounds in Zone 4 in greater than 95% yield. My research has also involved optimizing each of the steps in our synthetic pathway to improve upon the overall purity and yield of these novel compounds.



# Biological Evaluation of the Anticancer Activity of a Novel Class of Benzisoxazolo[2,3-a]pyridinium and Benzisoxazolo[2,3-a]quinolinium Compounds

Hua-Wu Huang (2014)

Mentor: Dr. Takita Felder Sumter  
Dr. James Hanna

While the initiation and development of cancer results from the deregulation of hundreds of genes and signaling cascades, most conventional chemotherapeutic agents are associated with nonspecific interactions that lead to adverse side effects. Accordingly, the need for low molecular weight inhibitors that disrupt DNA-dependent cellular events remains. We previously investigated the activity of a small library of novel benzisoxazolo[2,3-a]pyridinium (Figure 1) compounds against HCT116 colon cancer cells and recorded activity in the low to mid-micromolar range. The small planar structure of these novel compounds is a key structural feature of a number of DNA binding drugs and was explored as a mechanism by which these compounds act. DNA binding to most potent compounds was assessed using molecular docking studies and Hoechst 33258 fluorescence competition assays. In agreement with *in silico* simulations, the results of DNA binding assays of the compounds competing against minor groove binder Hoechst 33258 suggest direct DNA interactions. In fact, when benzisoxazolo[2,3-a]quinolinium (Figure 1) compounds were included in the studies, we observed binding affinities comparable to the chemotherapeutic drug, ellipticine. These findings prompted the biological evaluation of benzisoxazolo[2,3-a]quinolinium analogs of the most potent pyridinium compounds. All quinolinium analogs evaluated exhibited good activity against HCT116 colon cancers cells, although marked improvements in anticancer activity were not observed. When evaluating the impact of substituent position on activity, there seemed to be a relationship between substituent position and antitumor activity although additional studies are required. In all cases, activity was comparable to common anticancer compounds. The novel class of compounds all exhibit reasonable antitumor activity and serve as starting points for a new series of cytotoxic compounds with the benzisoxazolo[2,3-a]pyridinium or quinolinium core.

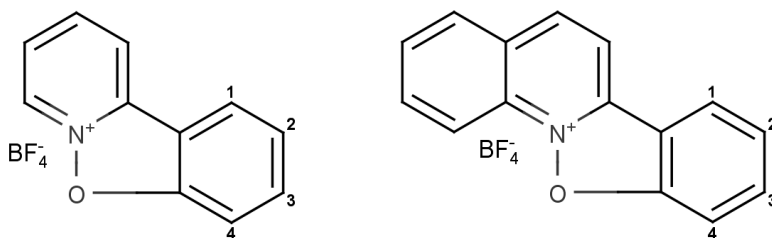


Figure 1. Chemical structures of benzo[4,5]isoxazolo[2,3-a]pyridinium tetrafluoroborate (left) and benzo[4,5]isoxazolo[2,3-a]quinolinium (right) parent compounds.

*This work was supported by grants from the NCI (1R15CA137520-01 and NIGMS(8 P20 GM103499) of the National Institutes for Health.*

## Synthesis of a Thiazacrown Ligand for the Quantification of Cu (I) Binding Interactions Under Aqueous Conditions

Mattie Ingersoll (2013)

Mentors: Dr. Nicholas Grosseohme  
Dr. James M. Hanna

Copper (Cu) is essential in many of the human body's natural systems. The average person can generally maintain regular Cu levels by eating a balanced diet and living a healthy life; however, various medical conditions exist that can disrupt the concentrations of Cu in the body: Menkes Kinky Hair Syndrome, Wilson's Disease, and Osteoporosis. Copper deficiency may lead to problems with connective tissue, muscle weakness, low blood cell count, and paleness. On the other hand, too much Cu can lead to copper toxicity, which happens when excess copper builds up in the liver, overflows into the body, and reaccumulates in the kidneys, brain, and eyes. Recent research also links copper accumulation to brain diseases like Alzheimer's and Parkinson's. The need to quantitatively observe copper concentrations in the body is clear, but researchers have recently demonstrated that previous in-vitro experimentation with copper has focused on the wrong oxidation state, Cu (II). Of copper's two states, Cu (I) is far more physiologically relevant than Cu (II); unfortunately, Cu (II) is immensely favored in the aqueous and aerobic environment of the human body. New experimentation aims to observe the binding interactions of Cu (I) specifically, but the disproportional oxidation state equilibrium makes the task challenging. The aerobic condition can be eliminated, reducing the concentration of Cu (II), by working in an anaerobic glove box, but the oxidation state equilibrium of the aqueous condition still results in a Cu (I):Cu (II) ratio of 1:1000. To further manipulate copper's oxidation equilibrium, ligands may be used to secure copper atoms in the proper oxidation state. To hold copper in the +1 oxidation state, a ligand must be capable of surrounding an entire copper atom and binding to all four binding sites. Securing copper in the +1 state with a ligand will remove that atom from the equilibrium and will force an aqueous Cu (II) atom to be converted to Cu (I). Our lab's goal is to synthesize such a ligand, enabling future experimentation with Cu (I) to be much more effective and successful. Our lab also strives to prove that our hypothesized ligand may be synthesized in an undergraduate laboratory with minimal access to chemicals and robust restrictions. Towards this end, we have successfully performed the first three steps of our proposed synthesis, as depicted below. We achieved a percent yield of 99 % for the first intermediate, 83% for our second, and 72% for our third, confirming the identity of each compound through mass spectroscopy and proton hydrogen nuclear magnetic resonance spectroscopy.

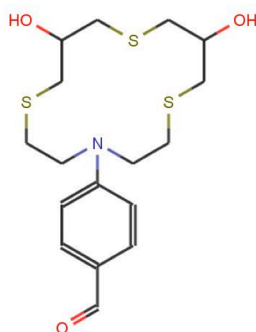


Figure 1: Thiazacrown ether ligand proposed to use for Cu(I) stabilization under aqueous conditions.

Support for this research was provided by the Winthrop University Research Council (SC130007), SC INBRE II, and the Winthrop University Department of Chemistry, Physics and Geology.



## **The urokinase and protein C systems in prostate cancer invasion and angiogenesis**

**Grace Jones**

**Mentor: Dr. Laura Glasscock**

In America, 1 in 6 men will be diagnosed with prostate cancer in 2013 (Siegel et.al.). The progression of prostate cancer is dependent on angiogenesis and tumor cell invasion. Both prostate cancer and endothelial cells are capable of producing similar proteins for various functions. Three of these proteins are urokinase type plasminogen activator (uPA), plasminogen activator inhibitor I (PAI-1), and activated protein C (APC); all of which are present in coagulation and implicated in tumor progression, specifically in invasion and angiogenesis. uPA's promotion of angiogenesis and invasion is well documented but its activity in the presence of APC and PAI-I is unknown in prostate cancer. Due to their known functions in coagulation, we hypothesized that uPA and APC alone increase both invasion and angiogenesis, that PAI-1 alone has no effect on invasion and angiogenesis and that PAI-I will inhibit both APC and uPA induced invasion and angiogenesis. However, we further hypothesized that in the presence of all three proteins, a more physiological scenario, PAI-I inhibits APC and allows uPA to resume its pro-invasive and –angiogenic activity. To study angiogenesis, we established an in vitro microtubule formation assay using a new endothelial cell line in our lab and determined that the ideal conditions for this assay are a low passage number, reduced growth factor Matrigel and a cell count of 30,000 cells per well. We determined that uPA increases microtubule formation and that PAI-1 alone has no effect, as expected. We are currently determining how APC alone and uPA, PAI-I and APC together affect microtubule formation. To study invasion, we set up an in vitro modified Boyden invasion assay using PC3 prostate cancer cells. The ideal conditions used for this assay were determined to be growth factor reduced Matrigel with serum free media, an incubation time of 16-20 hours and an optimal cell count of 1 million cells per well. We verified that uPA increases the invasive ability of PC-3 cells in our system and we are currently investigating how APC and PAI-1 affect invasion.

*Support for this research was provided by the NIH INBRE grant and McKay Urology Endowment Fund*



## Hydrothermal Investigation of CaCO<sub>3</sub>

Taisha S. Jones (2014)

Mentor: Dr. Maria C. Gelabert

Hydrothermal synthesis is a method that uses hot, pressurized water to crystals, and for this research, the hydrothermal method was used to produce calcium carbonate. Some of the experiments for this research used a calcium ion complexing agent, such as ethylenediaminetetraacetate (EDTA), L-tyrosine, DL-aspartic acid, L-lysine and L-cysteine, and the molar ratio for complexing agent to calcium was varied. For the experiments not using a complexing agent, pH was investigated. The morphology and the supersaturation value for the product was determined using microscopy and OLI Systems speciation software. Supersaturation  $\sigma$  can be defined as the ratio between molality of a specific ion with ligand,  $m_L$ , divided by the molality in a saturated solution  $m_0$ , such that

$$\sigma = \frac{m_L}{m_0}$$

Supersaturation values larger than 1 should result in a precipitate and values less than 1 yield no precipitate. Further, supersaturation values closer to 1 generally result in larger crystals compared to supersaturation values that are much larger. The table below shows the OLI-calculated supersaturation for Ca<sup>2+</sup> with different ligands. The blue areas represent the samples with no precipitate. The saturation values for the samples without ligand decreases as the pH increases, and imaged crystals correlate with an increase in size as pH increases. With the amino acid experiments, average supersaturation value for DL-aspartic acid was higher than the average value for the samples that used L-lysine, and the corresponding crystals for aspartic acid are smaller. In summary, experiments with no ligand and a few different amino acids demonstrate that crystal sizes vary inversely with supersaturation, consistent with crystal growth theory.

	90 °C		Room temperature	
	1:1	2:1	1:1	2:1
No ligand (pH 7)	48.55			
No ligand (pH 8)	45.65			
No ligand (pH 9)	38.32			
EDTA (pH 5.4)	1.087			
EDTA (pH 8)	0.04624	26.8		
L-tyrosine	7.701	7.677	8.380	8.202
L-lysine	7.942	7.833	8.285	3.932
DL-aspartic acid	8.565	8.141	8.569	8.237

Table. Supersaturation for Ca<sup>2+</sup> calculated with OLI speciation software at two investigated temperatures, with ligand:Ca<sup>2+</sup> molar ratios indicated. Blue areas indicate formation of no precipitate and gray areas are unexplored conditions.

*Support for this research was provided by SAN EPSCoR/IDEA, College of Arts and Sciences Faculty Startup Funding and the Winthrop University Department of Chemistry, Physics and Geology.*



## The Effects of Clioquinol on Amyloid- $\beta$ Oligomer Distributions

Kristen McLaurin (2014)

Mentor: Dr. Robin K. Lammi

Amyloid- $\beta$  ( $A\beta$ ) is a protein of 39-43 amino acids that self-associates into a diverse array of neurotoxic aggregates linked to Alzheimer's disease (AD). Recently, the smallest  $A\beta$  oligomers, dimers and trimers, have been shown to cause memory deficits when they are recruited to the synapse, perhaps due to zinc release during neurotransmission. Last summer, we used single-molecule fluorescence methods to understand how zinc binding affects dimer structure and to determine whether metal-induced changes are reversed upon chelation with clioquinol (CQ). We found that zinc binding has small but noticeable effects on observed dimer structures; perhaps more significantly, it also restricts the ability for dimers to undergo structural change, which may facilitate further aggregation. Furthermore, addition of clioquinol only partially reverses the changes caused by zinc. This summer, we completed a single-oligomer analysis to investigate whether clioquinol inhibits  $A\beta$  association in metal-free conditions, as another group has proposed. Measurements were performed using  $A\beta$ 40 peptides labeled at the N-termini with FAM dye and at the C-termini with Lys-biotin moieties to permit tethering to functionalized cover slips. Peptide species were classified as monomers, dimers, trimers, or polymers based on the number of photobleaching steps observed in their fluorescence intensity profiles. Distributions of peptide species were determined for metal-free samples in the presence and absence of excess clioquinol (10 equiv.). T-tests (unequal variance) were used to compare results for individual samples in each environment. In all cases, very high  $p$ -values were obtained, indicating that the distributions of peptide species were statistically indistinguishable. This is also evident in the ensemble distributions below (Figure 1), which depict the combined results for all six samples studied (three for each environment of interest). Therefore, our findings suggest that clioquinol does not inhibit or reverse  $A\beta$  association under metal-free conditions. Collectively, this work provides new insights into the role of zinc in promoting  $A\beta$  association and the utility of metal chelation as an approach for AD prevention and treatment.

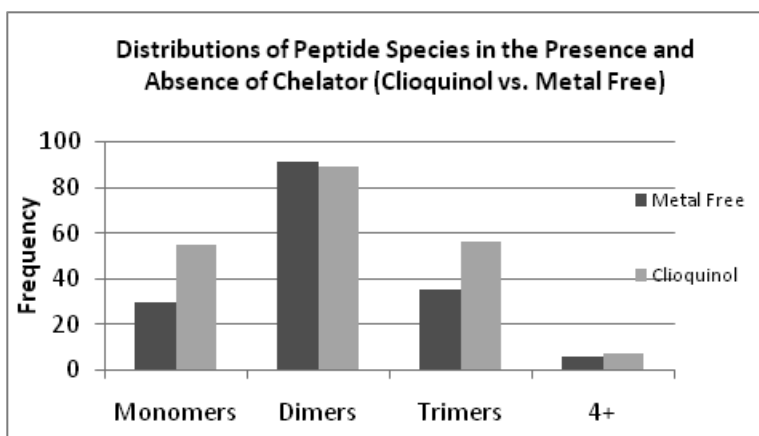


Figure 1: Ensemble distributions of  $A\beta$  peptide species in the absence ("Metal Free") and presence ("Clioquinol") of 10 equiv. of CQ. Each distribution represents the combined results of three separate samples. Statistical analyses of sample and ensemble distributions confirm that excess clioquinol has no significant effect on  $A\beta$  oligomerization in metal-free samples.

*Support for this project was provided by an RUI grant from the National Science Foundation (CHE-0848824).*



## Characterization of the Iron Regulator RitR from *Streptococcus pneumoniae*.

Jesse McLaughlin (2015) and  
Ashley Williams (2016)

Mentor: Dr. Nicholas Grosseohme

Iron serves a major role in the catalytic production of cytotoxic reactive oxygen intermediates. Due to this interaction being harmful to organisms, bacteria have evolved mechanisms that are able to minimize iron-based toxicity. One such mechanism is the Regulator of Iron Transport (RitR) in *S. pneumoniae*. This protein has been identified as a strong repressor of pneumococcal iron uptake (*piu*) transporter synthesis in *S. pneumoniae*. While this iron regulatory network has yet to be characterized, it is known that RitR functionally interacts with a Eukaryotic-like Serine-Threonine kinase phosphatase pair, StkP and PhpP respectively, which, like RitR, have been associated with DNA repair, iron uptake, and oxidative stress. We hypothesized that iron binds directly to the Receiver Domain (RD) of RitR in the event that there is an abundance of intracellular iron, preventing the activation of the *piu* operon. We also hypothesize that this protein becomes phosphorylated by StkP and dissociates itself from the *piu* promoter region to activate iron uptake in the event that there is no excessive iron within the cell. To date, we have successfully cloned RitR (both full-length and DNA binding domain, DBD), StkP, and PhpP, expressed the proteins in *Escherichia coli* cells, and purified them using a series of chromatographic procedures. Once purified, experimentation involving *piu*DNA, RitR full-length, and RitR-DBD was conducted to characterize the interaction that the protein-DNA complex had with an active kinase domain, as well as in the presence of iron. We are currently in the process of conducting further DNA-binding experiments to fully characterize the iron regulatory network of RitR in *S. pneumoniae*.

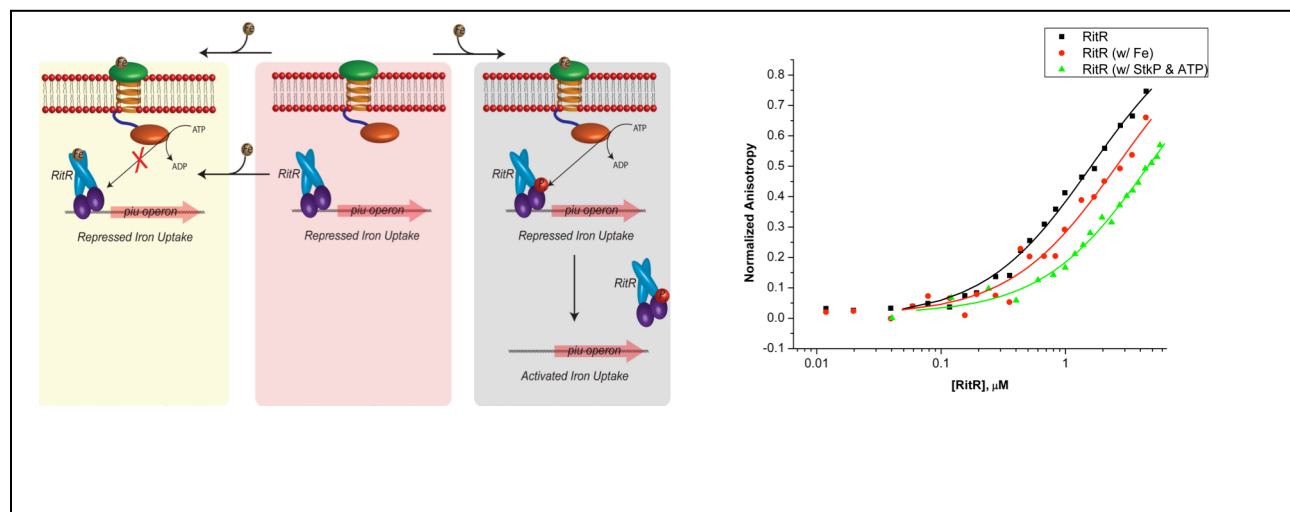


**Figure 1: A: Summary of known and hypothesized RitR function. Generally, RitR responds to an extracellular signal that propagates through an activated kinase. Upon activation, the kinase phosphorylates RitR, in an ATP-dependent manner, preventing RitR from repressing iron uptake machinery. We hypothesize that RitR can directly sense intracellular iron, a feature that seems necessary to prevent excessive iron accumulation in the presence of iron-rich growth conditions. B: Representative DNA-binding data testing this hypothesis.**

Support for this research was provided by an EPSCoR GEAR:RE Grant and the Winthrop University Department of Chemistry, Physics and Geology.



## Cloning of a novel GH30 Endoxylanase from *Bacteroides vulgatus* for X-ray Crystallographic Analysis

**Briana Milks (2016)**

**Mentor: Dr. Jason C. Hurlbert**

The principle objective of this research is to solve the structure of a *Bacteroides vulgatus* Glycosyl Hydrolase Family 30 subfamily F xylanase (BvGH30) identified by amino acid sequence analysis of the GenBank database. This family of enzymes is unique in that its members have a substrate specificity pocket that determines the type of xylan substrate that can be degraded. Different xylans from different plant types have different monosaccharide substitutions on the main polymeric chain. Sequence alignments were done to compare BvGH30 to other subfamily F xylanases, and differences in the amino acids that form the substrate specificity pocket were detected. Determining the structure of BvGH30 will reveal how the xylanase substrate and will enlarge our understanding of the chemical mechanisms by which members of this family discriminate between different sugar substituents on the xylan chain. Such an understanding is of interest because it has potential to reveal unique enzymatic activities for the degradation of lignocellulosic biomass. A synthetic gene encoding BvGH30 was designed and obtained as source DNA for our experiments. A synthetic gene has the advantages of having codons that are specific for the *Escherichia coli* host used to express the gene and we could easily engineer a thrombin-cleavable amino terminal hexahistidine tag. The synthetic gene was received in a pUCIDT cloning vector unsuitable for use in protein expression trials, so the first step in this experiment was to cut the BvGH30 gene out of the pUCIDT vector backbone and ligate it into a pET 28b vector that would be used for expression trials. Once cloned into the pET28b vector, the next step in this research will be to express the protein which can then be purified and crystalized in order to collect the diffraction data and solve the structure.

*Support for this research was provided by a SC-EPSCoR GEAR:RE grant.*



## Synthesis, Purification and Analysis of Novel Zone 4 Sphingosine Kinase Inhibitors

**Louise Mount (2013)**

**Mentor: Dr. Christian Grattan**

Sphingosine Kinase I (SK1) is a lipid kinase that catalyzes the formation of sphingosine-1-phosphate. This enzyme has been found to be overexpressed in tumor cells causing the cells to proliferate instead of going through the natural cycle to apoptosis. Sphingosine Kinase is manifested from ceramidase converting ceramide to sphingosine, which is when the sphingosine kinase comes in and phosphorylates the sphingosine to produce sphingosine-1-phosphate. To stop this process from happening SK1 inhibitors are required. By way of a template molecule known to inhibit sphingosine-kinase 1 *in vitro*, we have designed novel derivatives hoping to improve both bioavailability and efficacy through improved interaction with the enzyme. This project involved creating different synthetic derivatives a naphthalene ring portion on the molecule. In its place, a simple phenyl ring was introduced with either a hydroxy or a methoxy group attached to either the second or third positions. By means of synthesis, purification and analysis it was found that these compounds were successful made. These compounds have yet to be tested for bioavailability and interaction with the enzyme which is the next step towards refining our template structure.



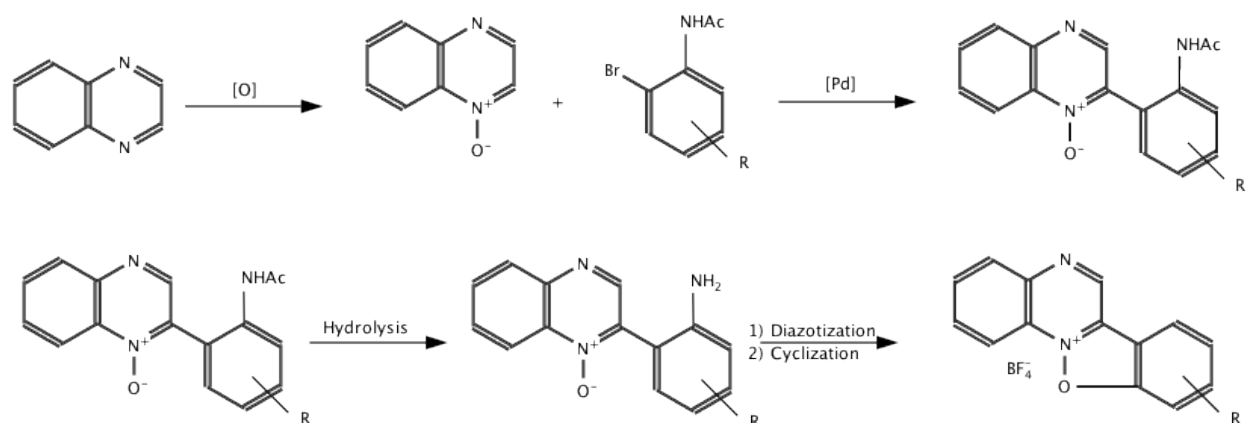


## Synthesis of Benzisoxazolo[2,3-*a*]quinoxalium Tetrafluoroborates

Jamie Risa Murakami (2015)

Mentor: Dr. James M. Hanna, Jr.

Recently, researchers in the Hanna lab synthesized several novel benzisoxazolo[2,3-*a*]azinium tetrafluoroborates and in collaboration with Dr. Takita Sumter, found that these compounds exhibited some activity against HCT 116 colon cancer cells. As part of a structure-activity study aimed at increasing the cytotoxicity of this new class of compounds, we are carrying out the synthesis of the quinoxalium analog via the pathway shown in the figure below.



Using a modification of the direct arylation of azine *N*-oxides introduced by Fagnou et al., we have attempted to affect substitution on quinoxaline *N*-oxide using methyl-substituted *o*-bromoacetanilides. Previous work in our lab found that the direct arylation of azine *N*-oxides was successful employing microwave heating; a ligand, palladium acetate (3:1, 5 mol % Pd); and potassium carbonate in toluene. Reacting quinoxaline *N*-oxide under these conditions using DIPET (di-isopropylphosphoniummethylammonium bis(tetrafluoroborate)) as the ligand with a 4- or 5-methyl substituted *o*-bromoacetanilide gave the desired product in yields ranging from 59 to 83%. Hydrolysis of the 4-methyl direct arylation product gave the aniline in 93% yield, which was smoothly diazotized and cyclized to the benzisoxazolo[2,3-*a*]quinoxalium tetrafluoroborate in 63% yield. However, during the hydrolysis of the 5-methyl direct arylation product, the desired aniline began to form according to GCMS, but prolonged heating seemed to cause product decomposition. This unexpected observation is currently under investigation in our lab. Upon development of a reproducible hydrolysis, additional methyl substituted *o*-bromoacetanilides will be reacted under direct arylation and then hydrolysis conditions. These compounds will then be cyclized and the resulting products evaluated for their anti-cancer activity.

*Support was provided by an NIH-INBRE grant from the National Center for Research Resources and the National Institute for General Medical Sciences, the Winthrop University Research Council, and the Winthrop University Department of Chemistry, Physics, and Geology*



## Cloning of a novel GH30 Endoxylanase from *Paenibacillus mucilaginosus* for X-ray Crystallographic Analysis

Briana Murray (2015)

Mentor: Dr. Jason C. Hurlbert

Xylanases are enzymes that hydrolyze the xylan chains in the hemicellulose of plant cell walls. The hemicellulose fraction of the plant cell wall is responsible for “gluing” together the cellulose fibrils that support the cell wall. Much research into the production of ethanol-based fuel sources by biocatalysts has centered on the production of enzyme that degrade the cellulose fraction of plant biomass, not the hemicellulose fraction, despite the fact that up to 30% of non-woody plant materials and 20% of woody plant material is composed of hemicellulose. Our research is focused on identifying and elucidating the chemical mechanisms by which enzyme degrade hemicellulose, a heretofore unused component of plant cell walls. Utilization of this material has the potential to significantly boost fermentative yields without diverting biomass from human or animal food chains, thereby preventing price spikes seen a few years ago when corn stocks were diverted to biofuels input streams. Endoxylanases are found in three distinct families of glycosyl hydrolase: Family 10, 11 and 30. Members of family 30 share a similar  $\alpha 8/\beta 8$  core structural fold with an attached carbohydrate binding domain. They are unique in their ability to degrade xylan substrates with chemical substituents attached to the polymeric xylose chain. There are 8 subfamilies (Labeled A through H) within the GH30 grouping, and the subfamily classification is based upon amino acid sequence identity. Recently, we have identified seven sequences that do not share significant sequence identity with any subfamily, which may mean that they represent a new, ninth subfamily. Our research intends to complete an x-ray crystallographic analysis of one of these new proteins, an endoxylanase from *Paenibacillus mucilaginosus*. The putative *Paenibacillus mucilaginosus* GH30 Subfamily I structural gene (PmGH30) was obtained from a commercial vendor who synthesized an *Escherichia coli* codon optimized gene bearing a cleavable, amino-terminal hexahistidine tag and two restriction endonuclease sites: NcoI and XhoI at the 5' and 3' ends of the gene, respectively. The plasmid was used to transform *E. coli* DH5 $\alpha$  cells in order to obtain large quantities of the DNA to work with. This DNA was then digested using the restriction endonucleases NcoI and XhoI, and the PmGH30 insert gene was isolated using an agarose gel extraction protocol. The same experiments were ran using *E. coli* pET28b, the target vector the extracted PmGH30 gene will be ligated into. Two sets of ligation reactions were performed using two different commercially supplied DNA ligases and buffers. The ligation reaction times were varied from 15 minutes to 18 hours (overnight), as were the ligation reaction temperatures, 16 C and 25 C. Both *E. coli* DH5 $\alpha$  cells and *E. coli* NovaBlue competent cells were transformed by the ligation reactions. To date, we have been unable to obtain any clones using either procedure. Future work will focus on the ligation reactions so as to develop an expression construct containing PmGH30. This expression construct will then be used to express the gene in *E. coli* cells and the recombinant protein obtained will be purified and used in crystallization trials.

*Support for this research was provided by a SC-EPSCoR GEAR:RE grant.*



## Purification and Characterization of the Nickel Uptake Regulator (NUR)

Denise Peppers (2015)

Mentor: Dr. Nicholas Grossoehme

*Streptomyces coelicolor* is a microorganism that is important in research for antibiotic production. In *S. coelicolor*, metal regulation is significant to maintain homeostasis within the cell. The Nickel Uptake Regulator (NUR) maintains levels of nickel within the cell. The goal of this research project is to purify NUR so that we may perform experiments to understand the relationship between DNA binding and metal binding to this protein. Our approach to this problem is to study the DNA and metal binding reactions independently using the wild type protein as well as a number of site-directed mutants. Results this summer were limited by unexpected hardships with obtaining protein of sufficient purity for metal and DNA binding assays.

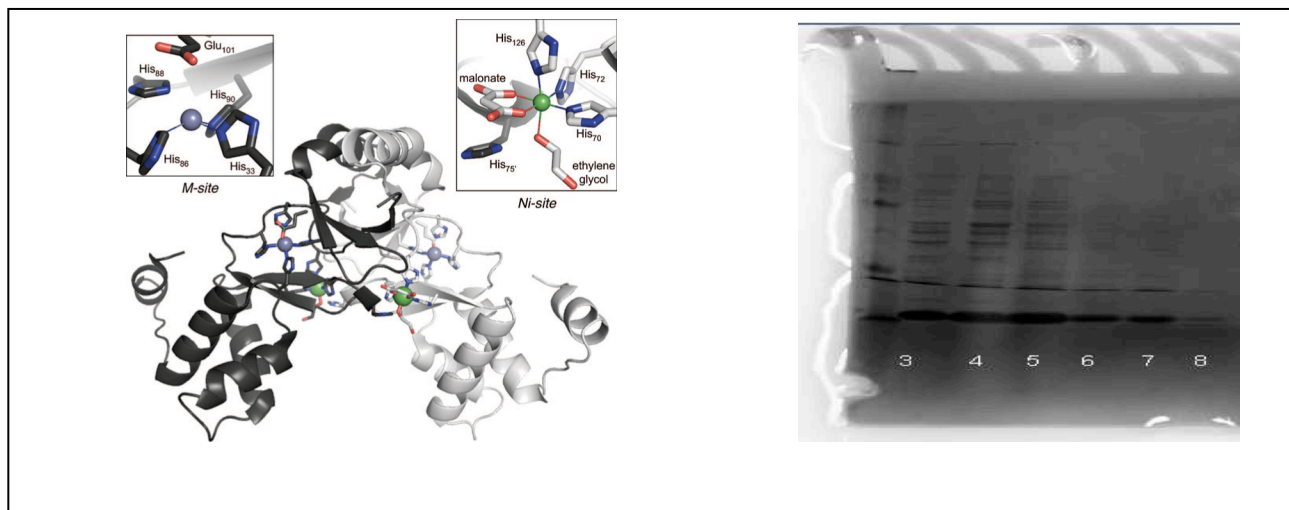


Figure 1: A. Structure of NUR with the two metal binding sites highlighted. B. SDS-PAGE gel of NUR after three chromatography steps.

Support for this research was provided by Research Corporation Grant (20160), Winthrop University McNair Scholars Program, and the Winthrop University Department of Chemistry, Physics and Geology.



## Combinatorics of quartet amalgamation

**Emili Price**

**Mentor: Dr. Joseph Rusinko**

One technique for reconstructing phylogenetic trees is inputting a set of quartets trees (containing four taxonomic units) and amalgamating them into a single supertree. We prove that the minimal number  $k(|X|)$  such that every compatible quartet system  $Q$ , with  $|Q| > k$  defines a unique tree is  $\binom{|X|}{4} - (|X| - 4)$ . Moreover, we prove that this bound is optimal because we can construct quartet systems of size  $\binom{|X|}{4} - (|X| - 3)$  that do not define a unique tree. We examine quartet subsystems to identify necessary and sufficient conditions required to ensure that the subsystems contain a sparse set of quartets meeting the criteria of Bocker for defining a unique supertree. We also prove a lower bound,  $p(|X|, n)$  for the percentage of time a unique tree will be reconstructed for any number of taxa and an arbitrary set of  $n$  quartets. Our technique can be applied to quartet tree amalgamation algorithms to increase the speed at which they construct supertrees.



## Expression, purification, and *ab initio* computation of structural models of the *Catenulispora acidiphila* GH30 xylanase

Alec Reed (2015)

Mentor: Dr. Jason C. Hurlbert

In today's international economic climate, fuel plays a key role in determining prices of goods and services. The development of an alternative source of biofuel that does not rely on edible portions of plant matter could help to alleviate some of the economic stress from both the fuel and food sectors of the economy. The ability to utilize non-edible sources of plant matter for biological fermentation to ethanol requires the use of new enzymes that can catalyze the depolymerization of the carbohydrate polymers such as xylan that can then be used as carbon sources by the biocatalyst. The GH30 xylanase from *Catenulispora acidiphila* (CaGH30) is one such enzyme, as it targets compounds in plant cell walls that are not digestible by humans. However, to be able to effectively utilize this protein, a determination of the structure is required to better understand its function. Our research has two distinct phases: A computation phase and a biochemical phase. In the computational phase, we have employed computational homology modeling with *ab initio* loop rebuilding to generate models of CaGH30 that will be used in molecular replacement phasing of x-ray diffraction data collected. In the biochemical phase of the work, we have cloned and expressed recombinant CaGH30 in *Escherichia coli*. We have developed a purification protocol that takes advantage of ion exchange, metal chelating affinity and gel filtration chromatographic methods. Our results indicate that significant amounts of recombinant protein were being expressed, but for some reason much of the protein is being lost during purification. Future work will entail attempting to purify the protein through alternate chromatographic methods or, if necessary, recloning of the structural gene encoding CaGH30 with placement of a removable hexahistidine tag on the amino-terminus.



Figure 3: Superposition of the five, lowest energy structures generated for CaGH30 after final loop rebuilding in Rosetta.

*Support for this research was provided by a SC-EPSCoR Scientific Advocate Network grant.*

## Silencing Cellular Expression of the *High Mobility Group A1 (HMGA1)* to Enhance Sensitivity to Chemotherapy

Derion Reid (2014)

Mentor: Dr. Takita F. Sumter

The overexpression and chromosomal rearrangements of the *High Mobility Group A1 (HMGA1)* gene are well-accepted hallmarks of various tumor types. The gene is alternatively spliced to yield two proteins, HMGA1a and HMGA1b, which play critical roles in transformation through mechanisms that are not well understood. Strong expression of *HMGA1* occurs during embryonic development but there is typically no expression in adult normal tissues. Most human neoplasias have elevated levels of *HMGA1* and its ectopic expression gene promotes malignant phenotypes *in vitro* and *in vivo*. Consistent with its oncogenic potential, HMGA1 is required for tumor-associated phenotypes in cancers including gastric, colon, prostate, and breast. In many tumors, *HMGA1* expression correlates with invasiveness confirming its potential as a prognostic marker. Mice bearing the *HMGA1* transgene develop intestinal polyps and the protein is overexpressed in mice bearing genetic truncations in the tumor suppressor, adenomatosis polyposis coli (*Apc*). These findings collectively suggest that HMGA1 proteins may act as cellular switches responsible for the conversion of normal colon tissues to the cancerous state. Moreover, overexpression of HMGA1 has been associated with resistance to certain chemotherapeutic drugs. The antineoplastic drug, 5-Fluorouracil (5-FU), is misincorporated into actively replicating DNA, eliciting DNA lesions and, eventually, death of colon cancer cells however; its clinical efficacy is often limited by the development of acquired drug resistance. We believe that overexpression of HMGA1 may enable cancer cells to become resistant to 5-FU's effects. To better understand the significance of HMGA1 in resistance to 5-FU, we used small interfering RNA targeting HMGA1 to determine if its knockdown influences sensitivity of colon cancer cells to 5-FU chemotherapy. We infected HCT116 cells with siRNA targeting *HMGA1* and quantitatively measured cell survival. Preliminary data suggests knockdown of *HMGA1* decreases HCT116 cell survival and current studies are underway to further characterize these findings. These findings may shed light on an additional pathway by which cancer cells circumvent the effects of anti-cancer therapy. It is possible that the molecular cross-talk between oncogenes and other cellular pathways can be better understood to better develop targeted therapies with decreased potential for resistance

*This work was supported by grants from the NCI (1R15CA137520-01 and NIGMS(8 P20 GM103499) of the National Institutes for Health, the National Science Foundation (MCB0542242) with student support from the Winthrop McNair Scholars program.*



## Expression and Purification of the *Xanthomonas gardneri* Protein Tyrosine Phosphatase, AvrBs7

Mariam Salib (2014)

Mentor: Dr. Jason C. Hurlbert

The protein tyrosine phosphatase AvrBs7 produced by *Xanthomonas gardneri*, is an effector protein that is essential for the bacterium to infect species of susceptible plants, which includes tomatoes and various pepper species. AvrBs7 is thought to function by disrupting a signal transduction pathway triggered by initial, extracellular phases of phytopathogenic attack, specifically degradation of the plant cell wall. In order to prevent the plant host from initiating a defense response, effector proteins, including AvrBs7, are injected directly into the plant cell by the bacterium via the Type III Secretion System. Once in the host, AvrBs7 binds to and dephosphorylates its target, thereby stopping the signal from being transduced and preventing the host cell from fighting the infection. In order to better understand the function of AvrBs7 and possibly design inhibitors for the protein, the atomic resolution structure of AvrBs7 must be determined via x-ray crystallography. Towards this end, we have begun purifying recombinant AvrBs7 in quantities suitable for crystallization trials. The coding sequence of *X. gardneri* AvrBs7 was cloned into pET21A (Amp<sup>r</sup>/C-terminal hexahistidine tag) which was used to transform *E. coli* NiCo (DE3) cultures. The resulting transformants were used to inoculate 6L of Luria-Bertani medium which were grown at 37°C to an optical density at 600nm of 0.6, were induced by the addition of IPTG and then grown for 18 hours post-induction. The cultures were harvested by centrifugation and the recombinant AvrBs7 was purified via a two-step procedure employing metal chelating affinity chromatography and gel filtration chromatography. Using this process, we obtained yields of less than 1 mg of purified AvrBs7 per liter of bacterial culture, far too low an amount to be used in crystallization trials. We are currently seeking to boost the yields of expressed protein by trying different hosts and growth conditions and hope to initiate crystallization trials once suitable expression conditions have been identified.

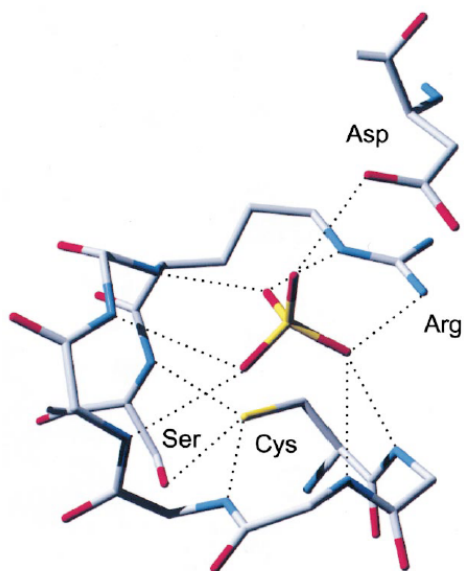


**Figure 1:** The P-loop: A hallmark active site motif found in protein tyrosine phosphatases (PTPs). The motif has the amino acid sequence: (H/V)CX<sub>2</sub>R(S/T) with the cysteine serving as the catalytic nucleophile initiating the dephosphorylation reaction by attacking the phosphorous of the substrate. Figure adapted from Kolmodin and Aqvist. (2001). The catalytic mechanism of protein tyrosine phosphatases revisited. FEBS Letters **498**: 208-213.

Support for this research was provided by the Winthrop University Research Council (SC13005).



## Machine learning for phylogenetic Invariants

**Hannah Swan**

**Mentor: Dr. Joseph Rusinko**

We build on Eriksson and Yao's work, which uses machine learning to optimize the power of phylogenetic invariants to reconstruct evolutionary trees. To do this, we solve a semidefinite programming problem, using GNU Octave and CSDP, a solver for semidefinite programming problems. Our method includes inequalities arising from the study of the real points on the phylogenetic variety into the metric learning algorithm. Previous work focused on selecting a good set of invariants for the construction of quartet trees, we extend this work to more taxa by testing the accuracy on twelve taxa trees.





## Practicality of a Gradient Flow Method of Analysis and Comparison with Standardized Quantitative Methods of Analysis

Velma Tahsoh (2014)

Mentor: Dr. Clifton Calloway

Quantitative analytical chemistry deals with determining the amounts of substances to a high degree of accuracy. The three techniques commonly employed in analytical chemistry include calibration curve, standard addition and internal standard methods of analysis. Techniques used in any particular analysis depend on the substance, or analyte, in question and the other components in the sample. The applicability of each technique depends on duration, accuracy, precision and amount of sample available for each method. In short, calibration curve is the simplest and quickest method of analysis; standard addition corrects for potential matrix interferences in the sample; internal standard corrects for changes in analyte or instrument response over time. This research develops a “gradient flow analysis” scheme that combines all three techniques and theoretically assumes the advantages of each technique. Typical calibration curve, standard addition, and internal standard analysis methods require the usage of glassware (e.g. volumetric flasks and pipettes) and pre-hand preparations of solutions...a time-consuming step. Gradient flow analysis uses three syringe pumps to dynamically create solutions with instrumental measurements using a flow cell (Figure 1). A single standard solution containing a known concentration of analyte and known concentration of an internal standard is prepared. With standard solution in one gradient syringe pump, solvent in the second gradient syringe pump, and sample in the third, constant flow syringe pump, the liquids combine and mix, then flow to the spectrophotometer cell. Simultaneous measurements of the analyte and internal standard signal allow rapid determination of the unknown concentration. In order to contextualize the efficiency of gradient flow analysis, the three standard methods were examined for precision and repeatability in the quantification of FD&C blue concentration in Listerine mouthwash. The precision of each standard technique was expectedly high, whereas gradient flow analysis could not be relied upon to produce repeatable results. The rest of the research time was dedicated to finding ways to improve the gradient flow results. When factors such as wavelengths, instrument parameters, and standard solution concentrations were varied, trial analyses results improved. Further laboratory research could improve efficiency of flow analysis and results and expose its potential to be standardized.

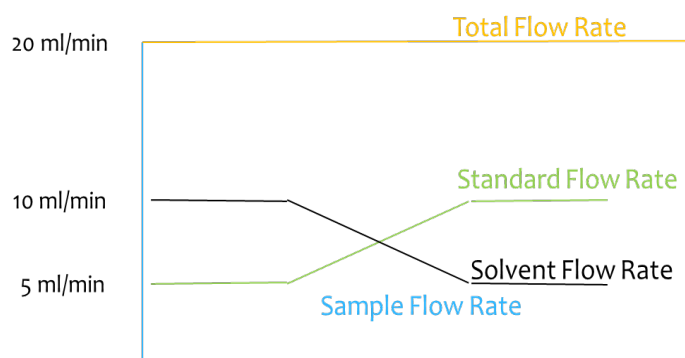


**Figure 1: Gradient flow analysis.** One syringe carries the standard solution, which is a known mixture FD&C Blue 1 analyte and FD&C yellow 5 internal standard. As the standard flow rate increase, the solvent syringe flow rate decreases, such that the total flow rate remains constant. The ratio of analyte to internal standard signals plotted against the reciprocal of the internal standard concentration yielding a linear result with a slope & intercept proportional to the analyte concentration.

*Support for this research was provided by the South Carolina EPSCoR Scientific Advocate Network (SAN) and the Winthrop University Department of Chemistry, Physics and Geology.*



## ***In vivo* confirmation of LPA's role in axon guidance by the inhibition of autotaxin using siRNA in embryonic chickens**

**James Vinton (2014)**

**Mentor: Dr. Eric Birgbauer**

The main principle of axon guidance is to investigate the role of chemical cues in the guidance and termination of growing nerves, both during development and after injury. Lysophosphatidic acid (LPA) is a bio-active lipid that has exhibited characteristics, such as growth cone collapse and neurite retraction, of an axon guidance molecule *in vivo*. LPA is produced endogenously by the exo-enzyme autotaxin (ATX). Based on previous research, during certain stages of chicken development, autotaxin is expressed posterior to the optic tectum. Retinal ganglion cell axons grow to and terminate at the optic tectum during the same stages of development that the expression of ATX was discovered. These findings suggest the possibility that the presence of autotaxin and the subsequent production of LPA could create a chemical barrier preventing the growing RGC axons from growing beyond the tectum. In order to confirm LPA's role in axon guidance *in vivo*, we obtained an siRNA for chicken autotaxin from Dr. Ohuchi in Japan. The ATX siRNA construct was cloned into an RCASB-GFP retroviral vector and transfected into a DF-1 cell line. The resulting virus was collected, concentrated using high speed centrifugation, and titered to determine efficiency. In order to test our hypothesis *in vivo*, experimental techniques and data acquisition procedures needed to be optimized. We determined, based on previous studies, the appropriate technique for the *ex ovo* culturing of embryonic chick embryos until E12 using embryo culture cups. Additionally, we successfully injected the control virus into the midbrain of E2 chick embryos and were able to confirm viral expression and further infection 5 days later. Furthermore, we were able to label the growing RGC axons of E6 chick embryos and detect the dye two days later as the axons were beginning to grow toward the optic tectum. Currently our results are promising; however, our data detection techniques still require further optimization. In the future, we would like to be able to inject both the control and ATX virus into the midbrain of the embryonic chick at E2, incubate them until E12, and using 3D rendering detect any abnormalities in the termination, growth, or response of the RGC axons as they transverse to the optic tectum. If our experiment can confirm LPA as an axon guidance molecule, it could potentially lead to pharmacological or developmental studies in the areas of nerve regeneration and blindness.

*Support was received from Winthrop University and from a National Institute Health Grant from the National Center for Research Resources for the support of the program entitled "South Carolina IDeA Networks of Biomedical Research Excellence" (SC-INBRE)*



## Synthetic Processes of Gold Nanosphere and Nanorod Particles for the Enhancement of Solar Cells

Justin Waller

Mentors: Dr. Prashant Kamat  
Dr. Clifton Harris

Gold nanospheres (NS) and nanorod particles (NR) were synthesized for the application to solar cell devices in order to enhance light absorption abilities and improve solar cell efficiency in energy conversion of solar light to electricity (Fig 1). These materials were designed to be incorporated in solar cell devices that display absorption compatibility between the metal particles and the sensitizer. When coupled with certain shape differentiated metallic particles, the absorbance of the solar cell in the wavelength range of the surface plasmon resonance (SPR) of the metal is enhanced, leading to higher flux of free charge carriers. Tailoring the size and shape of these particles directly correlates to the maximum wavelength of the SPR peak, as illustrated in figure 2. Gold (NS) particles were synthesized via sodium citrate reduction method and seed mediated growth methods, while gold (NRs) were synthesized via seed mediated growth methods only. Particles were layered with silica coatings of various shell thicknesses to prevent unwanted electron transfers and hole/electron recombination succeeding the excitation of the solar cell system instigated by solar light.

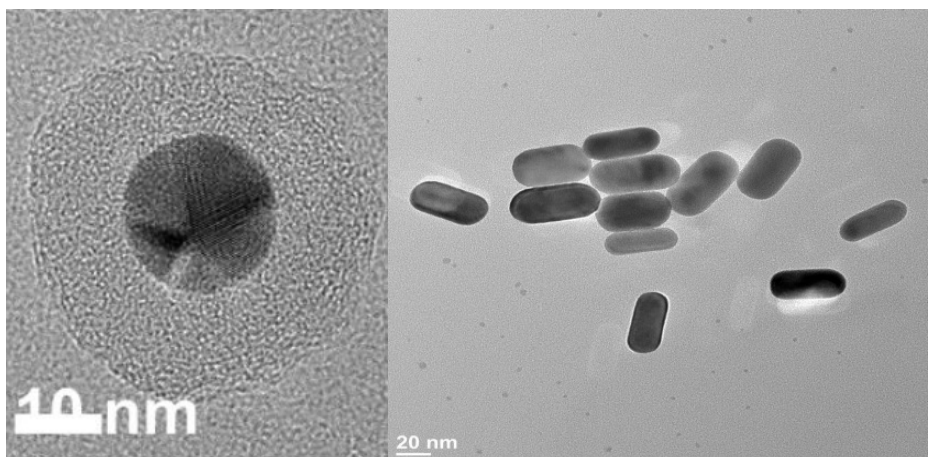


Figure 4. (Left) TEM image of citrate-capped Gold NS. (Right) TEM image of ascorbic acid functionalized Gold NRs.

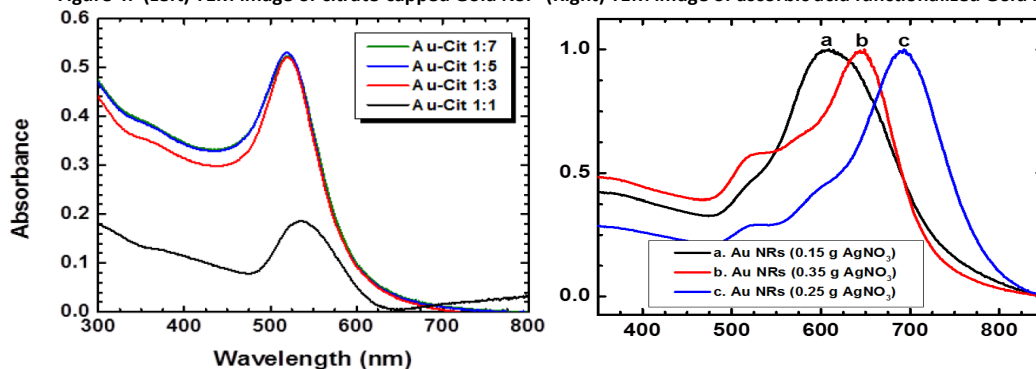


Figure 5. UV-Vis Absorbance Spectra of Gold NS (left) and NR (right) with various ratios of precursor to capping agent.

*This research was supported by the Graduate School of the University of Notre Dame and the U.S. Department of Energy*



## Synthesis and Evaluation of Biphenyltetrols as Amyloid- $\beta$ Aggregation Inhibitors

Sarah Wicks (2015)

Mentors: Drs. James M. Hanna, Jr. and Robin K. Lammi

The aggregation of amyloid-beta ( $A\beta$ ) to a  $\beta$ -structured aggregate is thought to be neurotoxic to nerve cells, therefore the prevention of monomers from associating to form complex secondary structures may be therapeutic for patients of Alzheimer's Disease. We have previously synthesized and evaluated biphenyl-3,3',4,4'-tetrol (3,4-BPT) as an efficient inhibitor of  $A\beta$  aggregation at stoichiometric levels. To aid our understanding of the hydrogen bonding interactions occurring between  $A\beta$  and 3,4-BPT, we synthesized several isomeric biphenyltetrols which were evaluated for their efficacy toward inhibition of  $A\beta$  aggregation. We have evaluated 2,3-BPT, 2,4-BPT, and 2,5-BPT as potential inhibitors at a 10X concentration by means of Thioflavin T assays and the results are shown below.

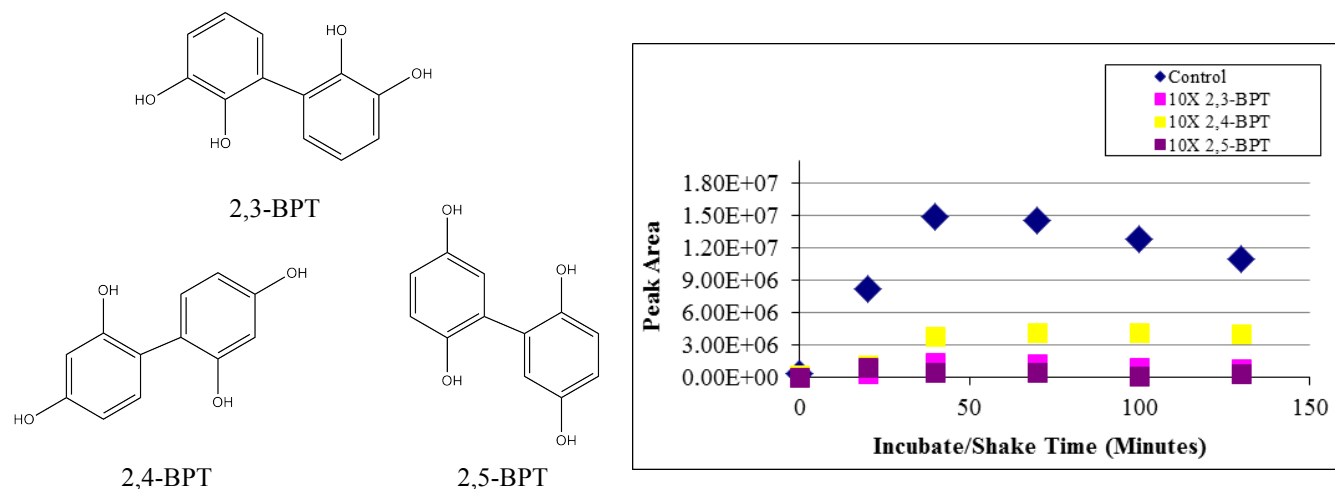


**Figure:** Structure of the biphenyltetrol isomers. The time course displays preliminary data of the inhibitory efficacy of evaluated isomers at a 10:1 inhibitor: $A\beta$  ratio (as compared to the inhibitor-free control).

The 2,3- and 2,5- isomers of BPT seemed to largely inhibit aggregation as measured by the Thioflavin T assay, while the 2,4-BPT was somewhat less effective. It appears that the arrangement of the hydroxy groups affects the extent of inhibition, perhaps by altering the way the inhibitor interacts with amyloid- $\beta$  through hydrogen bonding.

*Support was provided by the Winthrop University McNair Scholars Program and an NIH-INBRE grant from the National Center for Research Resources and the National Institute for General Medical Sciences.*